Quantum Image Encoding and Processing: A Comparative Analysis of Quantum Computing Systems

Michał Kordasz[1], Krzysztof Werner[1], Sundas Naqeeb Khan[1], Rafał Potempa[1]
Kamil Wereszczyński[1] and Krzysztof A. Cyran[1]

***Abstract*— In this work, the authors present a comparative analysis of quantum computers in the context of image processing. The benchmark was performed on seven quantum computers and one simulator. For the real quantum devices, three different families of QPU (quantum processing units) were used: ion-trap devices and superconducting qubits (the IBM Falcon and Eagle series). To encode 585 images on the quantum computers, the FRQI (Flexible Representation of Quantum Images) and LPIQE (Local Phase Image Quantum Encoding) methods were employed. The reconstructed images were compared using the MSE (Mean Squared Error) and PCC (Pearson Correlation Coefficient) metrics. The experimental protocol was implemented in Python, using the Qiskit, SciPy, and Geqie libraries. The results of the experiment are presented in tabular form, as histograms, and as a correlation matrix.**

This study investigated the correlation of MSE with (i) the QPU implementation technology (i.e., between ion-trap devices and superconducting qubits) and (ii) the type of superconducting quantum processor (Falcon vs. Eagle). Additionally, differences in the error distributions between these QPU series (Falcon vs. Eagle) were analyzed.

The main conclusions are as follows: a strong correlation of MSE with the type of superconducting quantum processor (Falcon vs. Eagle) and a moderate correlation of MSE with QPU implementation technology (ion-trap vs. superconducting) were demonstrated. Furthermore, it was shown that Falcon-series processors exhibit a bimodal error distribution, whereas Eagle processors exhibit a unimodal distribution. No correlation was found between MSE and the error rate.

I. Introduction

One of the contemporary branches of computer science is computer vision, which involves processing both single images and videos. With the development of quantum computing, quantum computers offer more efficient storage and processing capabilities for the increasing amount of data in computer vision. However, the physical limits of classical computer miniaturization, as described by Moore's law, have led researchers to explore alternatives like quantum computing. Despite being in the NISQ (Noisy Intermediate-Scale Quantum) era, quantum computers can already be used for image encoding methods such as FRQI. For instance, encoding a Full HD video of 1.5 hours at 30 frames per second would require only 43 qubits, which is feasible with current quantum hardware.

A. State of Art

The field of quantum image processing has gained significant attention as researchers explore its potential advantages over classical methods. Various studies have examined quantum computing systems and their applicability to image processing tasks, particularly in the NISQ era. There are approaches focus on hybrid quantum-classical models, demonstrating improved image classification and feature extraction capabilities through QSVM [1]. Comparative analyses of quantum processors have highlighted significant discrepancies in quantum image fidelity across different hardware platforms, with superconducting qubits outperforming ion-trap-based systems in certain tasks [2].

The authors aim to develop a comparative analysis of currently available quantum systems. This need is motivated by the lack of up-to-date comparative analyses of quantum systems.

The authors [3] note that there are no universal benchmarks for comparing quantum systems. However, they have presented general criteria for conducting a comparative analysis. Such a comparison must include the following features:

1) Representation of real-world problems.
2) Ease of adaptation and implementation.

In the report [4], the authors list existing methods for comparing quantum systems:

1) Average Gate Fidelity.
2) Process fidelity.
3) Quantum Volume.
4) Algorithmic Qubits.

However, all of these metrics are limited by their inability to compare different hardware architectures and native quantum gate sets. While we can measure the fidelity or the quantum volume of CNOT (controlled NOT) gates, this does not provide information about the capacity to execute a specific algorithm. Algorithmic qubits could, in principle, assess the suitability of a given algorithm for implementation on particular hardware, but they do not indicate the extent of architectural reconfiguration required to ensure competitive performance.

The authors hereby propose a benchmark based on:

- Comparing the fidelity of images obtained from quantum computers with the originals using the MSE and PCC metrics.
- The correlation matrix derived from the PCC results.
- MSE histograms for each of the quantum computers.

The approach presented for creating this benchmark remains useful for as long as the NISQ era endures. The authors contend that, as quantum technologies mature and the era of Fault-tolerant quantum computing arrives, benchmarks

[1]Silesian University of Technology, Gliwice, Poland michal.kordasz@polsl.pl

will be oriented toward computational power rather than examining noise, decoherence, and error rates in quantum computations, which are currently the dominant challenges in NISQ devices.

1) Are there a correlation between MSE and QPU implementation technology (i.e., between ion-trap and superconducting devices)?
2) Is there a correlation between MSE and the type of superconducting quantum processor (i.e., between the Falcon and Eagle series)?
3) Is there a difference in the error distribution between different QPU series (Falcon vs. Eagle)?
4) Is there a correlation between MSE and the Error Rate?

B. Contribution

The guidelines indicated by the authors [3] and [4] were used by the authors to create a comparative analysis in quantum computer vision, resulting in the creation of a benchmark for quantum systems. The comparative analysis was conducted on 7 different quantum devices and 1 simulator. For this purpose, 585 images were used. The following quantum systems were tested:

1) Falcon,
2) Eagle,
3) and an ion trap.

To encode images on a quantum computer, the FRQI [5] and LPIQE [6] methods were used. The choice of the FRQI method was dictated by the minimal use of qubits compared to other image encoding methods, such as IFRQI [7], MCQI [8], NCQI [9], NEQR [10], QRCI [11], or QUALPI [12].

Based on the obtained results, a statistical-comparative analysis was performed, using MSE and PCC comparative measures to compare the original images with those obtained from the quantum computer.

The execution of the experiment would not have been possible without the decomposition of multiply-controlled R_y gates. This was the first limitation the authors had to address in this work. Initially, for the decomposition of multiply-controlled gates, the authors employed a Gray-code–based decomposition [13] [14]. However, this approach also introduced constraints on circuit depth (i.e., the total number of gates), and ultimately the decision was made to use the Geqie library [15] for image encoding.

A comparative analysis of the images encoded on the quantum computers was then performed. To this end, the MSE and PCC metrics were applied to compare the original images with those reconstructed by the quantum devices.

In this section, the authors present state of the art, authors' contribution, and the structure of the paper. In Section II, the methodology is presented, including a description of the image-encoding method, the comparative metrics, and the quantum computers used in the study. Section III presents the results of the comparative analysis of the images obtained from the quantum computers. Finally, Section IV offers the conclusions and a summary of the work.

II. Materials and methods

A. Theoretical introduction

Quantum gates are operations that can be performed on qubits.

The mathematical construction of multi-qubit gates, such as the CNOT gate shown in Fig. 1, requires defining all the cases in which the gate will operate. This process is explained step by step in Fig. 1.

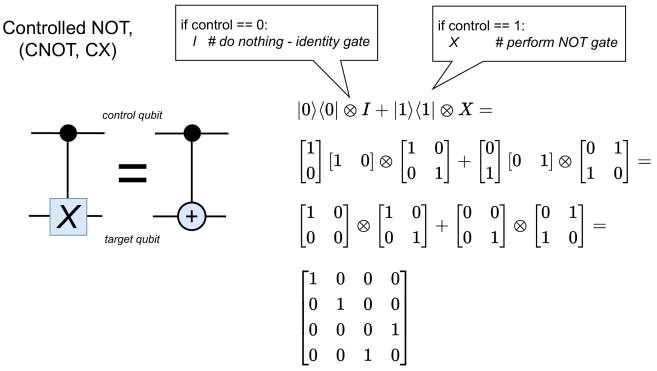

Fig. 1. Constructing mulitqubit gates — i.e. CNOT gate.

1) FRQI: It is a method used for encoding images on a quantum computer, leveraging its potential. The pixel intensity value is encoded as a superposition of black and white colors. The grayscale of a pixel (in the range $\langle 0, 255\rangle \in \mathbf{N}$) is mapped to the range $\langle 0, 1\rangle \in \mathbf{R}$. To achieve this, we use R_y gates.

$$|I(\theta)\rangle = \frac{1}{2^n} \sum_{x=0}^{2^{2n}-1} (\cos\theta_x |0\rangle + \sin\theta_x |1\rangle) \otimes |x\rangle \quad (1)$$

where:

$$\theta_x \in [0, \frac{\pi}{2}], x = 0, 1, \ldots, 2^{2n} - 1,$$

The FRQI method allows for efficient image storage and manipulation on quantum computers. By encoding the pixel values as quantum states, it is possible to perform parallel operations on the image data, which can lead to significant speedups in image processing tasks. The R_y gates are used to rotate the qubit states to represent the grayscale values of the pixels. This encoding scheme is particularly useful for quantum image processing algorithms, such as image compression, filtering, and pattern recognition.

One of the key advantages of FRQI is its ability to represent an entire image using a relatively small number of qubits. For an image of size $2^n \times 2^n$, only $2n$ qubits are required plus 1 for the grayscale. This compact representation is crucial for the practical implementation of quantum image processing algorithms on current quantum hardware, which has limited qubit resources.

2) LPIQE method: Let's consider an image of height H pixels and of width W represented by a matrix $I_m = \left[\hat{p}_{r,c}\right]_{H\times W} \wedge r \in \{0,\dots H-1\} \wedge c \in \{0,\dots W-1\} \wedge \hat{p}_{r,c} \in [0,1] \cap \mathbb{R}$, where $\hat{p}_{r,c}$ is the intensity of pixel placed in r-th row and c-th column. We can execute the (vertical) vectorization and obtain

$$\overrightarrow{I_m} = [p_j]^T, s.t. : j = rW + c \tag{2}$$

Using the *Encoding the constant data* (described in [6]) we can represent this form of an image with the state:

$$|I_m\rangle = \left[e^{ip_0}\dots e^{ip_J}, 0^{M-J}\right] = \sum_{j=0}^{J} e^{ip_j}|j\rangle, \tag{3}$$
$$J = WH - 1, \;\; M = 2^{\lceil log_2(WH)\rceil}$$

The first part of above state is the vector of WH exponential functions of pixels intensities, the second part is a complements to quantum state's requirement of having power of two coefficients. This exponential functions can be treated as local phases of a state, therefore we call it LPIQE. The state can be obtained by an operator defined by matrix:

$$\tilde{\mathcal{L}}(I_m) = \mathbf{1}\,\overrightarrow{I_m} = \begin{pmatrix} e^{ip_0} & 0 & \cdots & 0 \\ 0 & e^{ip_1} & \cdots & 0 \\ \vdots & & \ddots & \vdots \\ 0 & 0 & \cdots & e^{ip_J} \end{pmatrix}, \tag{4}$$
$$\mathcal{L}(I_m) = \left[\begin{array}{c|c} \tilde{\mathcal{L}}(I_m)_{J\times J} & \mathbf{0} \\ \hline \mathbf{0} & \mathbf{1} \end{array}\right]_{M\times M}$$

where $\mathbf{1}$ is an identity matrix / operator.

Hence this is operator that has on diagonal, the exponential e^{ip_j} of local phases being the intensities of pixels. It can be generated, on the low level of abstraction, using the combination of multi-controlled phase shift gates and the technique of uncomputation; however, currently available solution (e.g. Qiskit) provides tools for defining the operator as matrix, and the mapping it to the set of physically implemented gates. Therefore, we can conclude that such a definition of an operator is sufficient for current implementation.

3) Decomposition of Multiply-Controlled Gates: During the experiment, we encountered the problem of the inability to decompose multiply-controlled gates. In our case, the issue concerned the C^4R_y gate (a fourfold controlled R_y rotation gate). Therefore, a manual decomposition was necessary. An additional limitation was the restricted number of available qubits on some quantum systems, so a decomposition technique had to be chosen that did not require extra qubits (ancilla).

To achieve this, we used the technique proposed in [14], which utilizes a Gray code sequence [13].

B. Image comparison metrics used in this work

The following metrics were used to compare the similarity between images:

1) MSE [16].
2) PCC;

1) PCC: It is a metric which measures the relationship between datasets. This function returns the value in range $\langle -1, 1\rangle$, where -1 indicates full anti-correlation, and 1 indicates a full correlation of the datasets. Unlike MSE, PCC uses the range $\langle -1, 1\rangle$ to compare the similarity between images.

C. Quantum computers used in this work

For this study, the authors selected the quantum computers listed in Table I for benchmarking. Because remote access to quantum hardware incurs fees, the chosen devices were those whose combined usage costs fully exhausted the budget allocated to this project; accessing any additional machines on the market would have exceeded available funds. The careful optimization of the selection of QPUs in Table I thus made it possible to test the largest possible number of devices within the budgetary constraints. Unlike IBM—which provides its own Qiskit SDK (system development kit)—AWS (Amazon Web Services) offers the Braket SDK; to avoid code duplication, the authors used the Qiskit Provider for Amazon Braket.

TABLE I
QUANTUM COMPUTERS USED IN THIS WORK.

Quantum computer	Qubits	Quantum Volume	1Q gate error	2Q gate error	QPU
AWS Aria 1	21	N/A	0.05%	0.4%	Ions trap
IBM Simulator Statevector	32	N/A	N/A	N/A	simulator
IBM Brisbane	127	128	0.02%	0.7%	Eagle r3
IBM Kyoto	127	128	0.02%	0.7%	Eagle r3
IBM Lagos	7	128	0.03%	0.79%	Falcon r5.11H
IBM Nairobi	7	128	0.03%	0.79%	Falcon
IBM Osaka	127	128	0.02%	0.7%	Eagle
IBM Perth	7	128	0.03%	0.79%	Falcon r5.11H

1) Technology of the QPUs': The quantum computers used in this work are based on different technologies. The IBM QPUs (i.e. Falcon and Eagle) are based on superconducting technology, while the AWS quantum computer uses ion trap technology.

AWS Aria 1, by IonQ, is a 21-qubit quantum computer based on ion trap technology, utilizing $Yb-171^+$ atoms. Ytterbium atoms are first ionized and then placed in an ion trap created using oscillating voltage. All quantum operations, starting from initialization, are performed by manipulating the quantum states of the ions using lasers.

From the other hand, IBM quantum computers are based on superconducting qubits. The qubits are cooled to near absolute zero temperatures to reduce thermal noise and

decoherence. The qubits are manipulated using microwave pulses, and the quantum gates are implemented using superconducting circuits.

D. The experiment

For the experiment, 585 images were used. Additionally, for visualization purposes in the article, a photo from the cockpit of a Boeing 737 flight simulator was used (see Fig. 2). The images were encoded in the form of a unitary matrix on a quantum computer, then reconstructed and compared with the original in section III.

The image similarity metrics used in this work are MSE and PCC. The summary of the results is listed in Table II. All the code was written in Python using the Qiskit [17], Sci-kit image, and SciPy libraries.

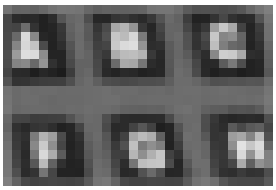

Fig. 2. Example image, used for experiment.

III. Results

Table II summarizes the comparison results of the obtained images against the original, for each quantum computer used in this study. Columns explanation:

- MSE,
- PCC,
- p-value - of PCC,
- STD - standard deviation.

Fig. 3 is a graphical representation of the results from Table II. The plot shows the results for each metric, i.e., MSE and PCC. The histograms given on Fig. 4 and 5 present the distribution of squared errors for each pair of images: original and reconstructed. Table III presents sigma intervals for the histograms, presented in Fig. 4 and 5.

The resulting images obtained from the various quantum computers are shown in Table 7 and 8.

Fig. 6 shows the PCC matrix between the images. Additionally, the following PPC were calculated:

- Ion trap vs IBM semiconductors QPU: 0.66,
- Falcon vs Eagle QPU: 0.72,
- MSE correlation to Error Rate: 0.07.

The resulting images obtained from the various quantum computers are shown in Fig. 7 and 8.

IV. Conclusions

The objective of this work was to conduct a comparative analysis of the maximum number of quantum computers that fit within the authors' budget. To perform the benchmark[1], seven quantum computers and one simulator were used. A

[1]Measure of the quality of something by comparing it with something else of an accepted standard

TABLE II
Comparison of statistics of retrieved images from quantum computers.

Quantum computer	MSE	PCC	p-value	STD MSE	STD PCC
Simulator Statevector	76.383	0.971	0	66.850	0.014
IBM perth	91.090	0.937	0	71.033	0.031
Aria 1	101.745	0.705	0	74.521	0.148
IBM kyoto	103.155	0.957	0	71.457	0.021
IBM nairobi	107.893	0.790	0	74.748	0.105
IBM lagos	110.468	0.837	0	77.677	0.082
IBM osaka	111.380	0.677	0	75.568	0.162
IBM brisbane	118.487	0.882	0	74.700	0.059

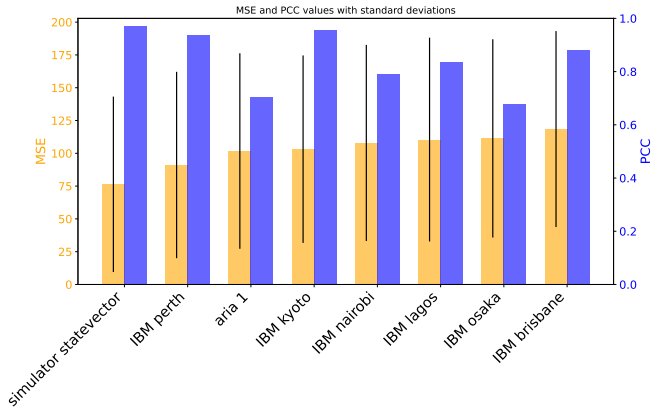

Fig. 3. Statistical comparison of quantum computers.

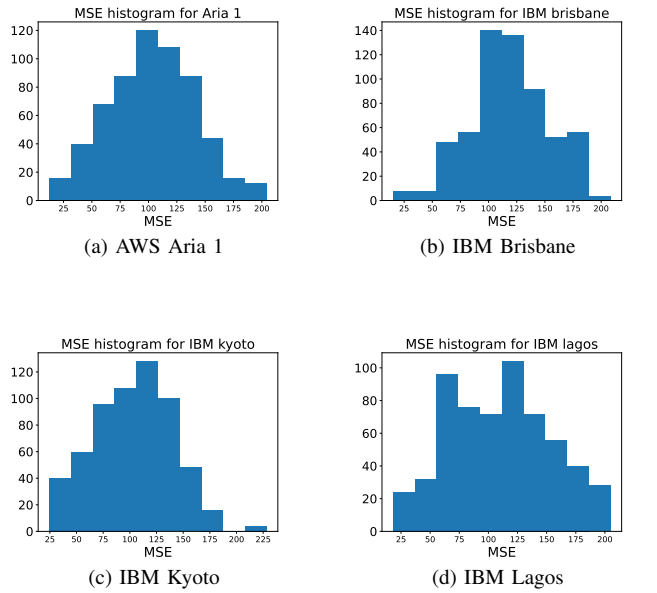

(a) AWS Aria 1 (b) IBM Brisbane

(c) IBM Kyoto (d) IBM Lagos

Fig. 4. MSE histograms of the images from various quantum computers (1/2)

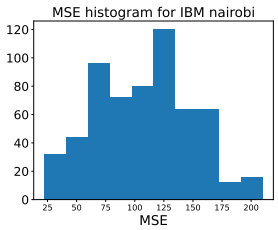

(a) IBM Nairobi

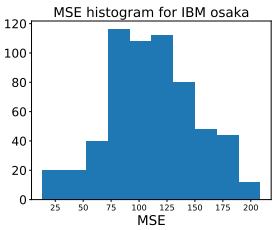

(b) IBM Osaka

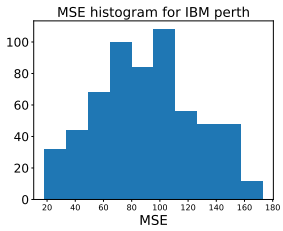

(c) IBM Perth

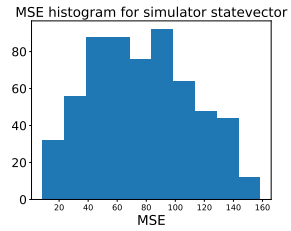

(d) IBM Simulator Statevector

Fig. 5. MSE histograms of the images from various quantum computers (2/2)

TABLE III

SIGMA INTERVALS FOR THE IMAGES

image name	1-Sigma Interval (%)	2-Sigma Interval (%)	3-Sigma Interval (%)
Aria 1	68.0	96.0	100.0
IBM brisbane	67.33	96.0	100.0
IBM kyoto	70.0	94.67	99.33
IBM lagos	64.67	98.0	100.0
IBM nairobi	64.67	95.33	100.0
IBM osaka	68.0	94.67	100.0
IBM perth	66.67	97.33	100.0
simulator statevector	65.33	98.0	100.0

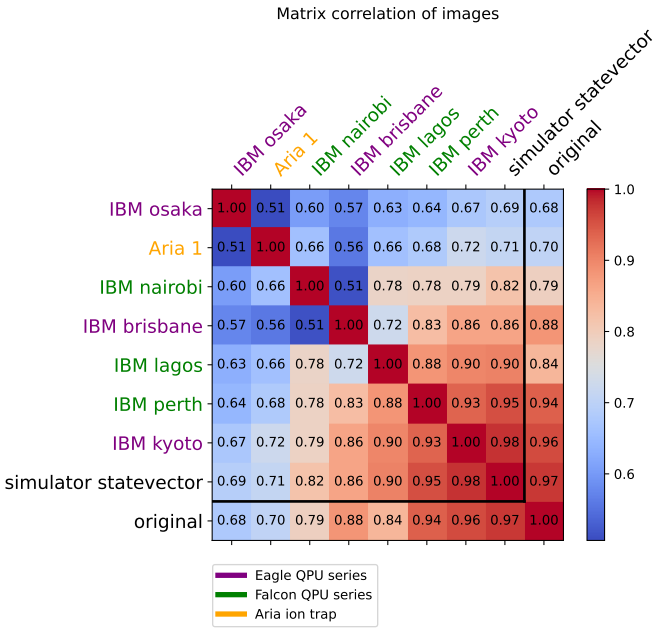

Fig. 6. Matrix correlation of images.

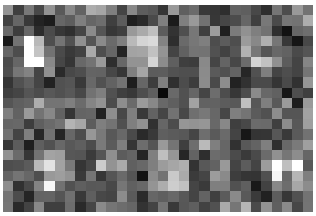

(a) AWS Aria 1

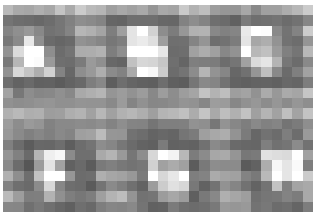

(b) IBM Brisbane

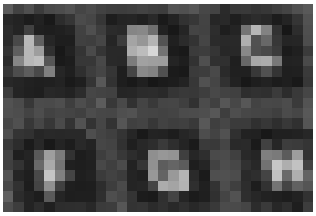

(c) IBM Kyoto

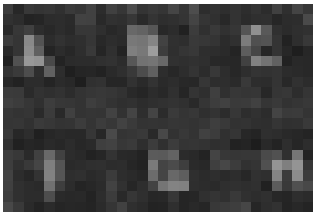

(d) IBM Lagos

Fig. 7. Images from various quantum computers (1/2)

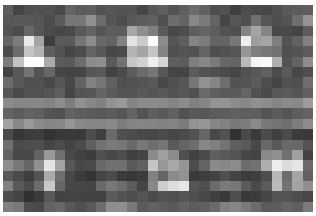

(a) IBM Nairobi

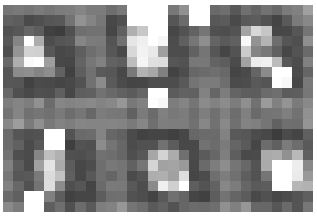

(b) IBM Osaka

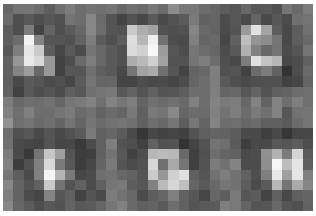

(c) IBM Perth

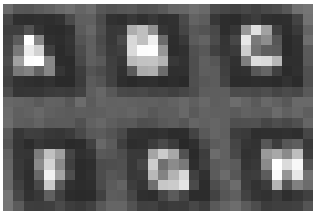

(d) IBM Simulator Statevector

Fig. 8. Images from various quantum computers (2/2)

total of 585 images were encoded on the quantum computers using the FRQI and LPIQE methods. To compare the images reconstructed from the quantum computers, the MSE and PCC metrics were employed. The experimental protocol was implemented in Python, utilizing the Qiskit, SciPy, and Geqie libraries. The results of the experiment are presented in tabular form, as histograms, and as a correlation matrix.

The research questions posed in this work were:

1) Is there a correlation between MSE and the QPU technology (i.e., between ion-trap and superconducting implementations)? — Yes; a moderate correlation of 0.66 was observed.
2) Is there a correlation between MSE and the type of superconducting quantum processor (i.e., between the Falcon and Eagle series)? — Yes; a strong correlation of 0.72 was found.

3) Is there a difference in the error distribution between different QPU series (Falcon vs. Eagle)? — Yes; Falcon-series processors exhibit a bimodal distribution, whereas Eagle is unimodal.
4) Is there a correlation between MSE and the Error Rate? — No; essentially no correlation (0.07).

Based on the results obtained in Section III the authors note that, as expected, the IBM Statevector quantum simulator achieved the best performance in terms of both MSE and PCC, which is consistent with the principles of the NISQ era.

It is worth highlighting that there is a moderate correlation between MSE and the underlying QPU technology. Images reconstructed on an ion-trap quantum computer, on average, exhibit lower fidelity than those reconstructed on superconducting-qubit machines, as evidenced by a PCC of 0.66.

An even stronger correlation (0.72) is observed between MSE and the specific type of superconducting quantum processor—namely, between the Falcon and Eagle series.

Examining the MSE results for the histograms shown in Fig. 4 and 5, one can see that the error distribution for the Falcon series is bimodal, whereas for the Eagle series it is unimodal. This suggests the possibility of classifying a QPU family based solely on the shape of its MSE distribution.

When addressing technical limitations, the authors encountered difficulties in decomposing multiply-controlled gates. One approach to overcome this is to decompose a multiply-controlled gate into multiple singly-controlled gates using Gray-code sequences. In this work, however, the Geqie library was employed to generate a single unitary matrix encoding the entire image.

Encoding images directly as a unitary matrix proves to be the most practical solution. In this scenario, the transpiler is responsible for converting the unitary into the native gate set of the target quantum device, thereby sidestepping the challenges associated with multiply-controlled gates.

The benchmark presented here directly tackles the challenges and constraints of NISQ-era quantum computers. The authors argue that, as fault-tolerant quantum computing emerges, new challenges and limitations will arise—necessitating the design of further benchmarks that incorporate criteria not yet available today.

ACKNOWLEDGMENT

The authors would like to acknowledge that this paper has been written based on the results achieved within the OptiQ project. This Project has received funding from the European Union's Horizon Europe program under grant agreement No 101080374-OptiQ. Supplementarily, the project is co-financed from the resources of the Polish Ministry of Science and Higher Education in the framework of the International Co-financed Projects program.

Disclaimer Funded by the European Union. Views and opinions expressed are, however, those of the author(s) only and do not necessarily reflect those of the European Union or the European Research Executive Agency (REA – granting authority). Neither the European Union nor the granting authority can be held responsible for them.

REFERENCES

[1] M. Shahid, M. A. Hassan, F. Iqbal, A. Altaf, S. W. H. Shah, A. V. Elizaincin, and I. Ashraf, "Enhancing movie recommendations using quantum support vector machine (qsvm)," *The Journal of Supercomputing*, vol. 81, no. 1, p. 78, 2024.

[2] P. Kulkarni, Sudhanshu, D. E. Huang, and E. W. Bethel, "From bits to qubits: Challenges in classical-quantum integration," arXiv e-prints, arXiv–2501, 2025.

[3] J. Wang, G. Guo, and Z. Shan, "Sok: Benchmarking the performance of a quantum computer," *Entropy*, vol. 24, no. 10, p. 1467, 2022.

[4] J. Kalloor, M. Weiden, E. Younis, J. D. Kubiatowicz, and I. Costin, "Towards a quantum hardware roofline: Evaluating the impact of gate expressivity on processor design," University of California, Berkeley, EECS Department, Tech. Rep. EECS-2024-78, 2024. [Online]. Available: https://www2.eecs.berkeley.edu/Pubs/TechRpts/2024/EECS-2024-78.html

[5] P. Q. Le, F. Dong, and K. Hirota, "A flexible representation of quantum images for polynomial preparation, image compression, and processing operations," *Quantum Information Processing*, vol. 10, no. 1, pp. 63–84, 2011.

[6] K. Wereszczyński, A. Michalczuk, D. Pęszor, M. Paszkuta, K. Cyran, and A. Polański, "Cosine series quantum sampling method with applications in signal and image processing," *arXiv preprint arXiv:2011.12738*, 2020.

[7] R. A. Khan, "An improved flexible representation of quantum images," vol. 18, no. 7, p. 201. [Online]. Available: http://link.springer.com/10.1007/s11128-019-2306-6

[8] H.-S. Li, Q. Zhu, R.-G. Zhou, L. Song, and X.-j. Yang, "Multi-dimensional color image storage and retrieval for a normal arbitrary quantum superposition state," vol. 13, no. 4, pp. 991–1011. [Online]. Available: http://link.springer.com/10.1007/s11128-013-0705-7

[9] J. Sang, S. Wang, and Q. Li, "A novel quantum representation of color digital images," vol. 16, no. 2, p. 42. [Online]. Available: http://link.springer.com/10.1007/s11128-016-1463-0

[10] Y. Zhang, K. Lu, Y. Gao, and M. Wang, "NEQR: a novel enhanced quantum representation of digital images," vol. 12, no. 8, pp. 2833–2860. [Online]. Available: http://link.springer.com/10.1007/s11128-013-0567-z

[11] L. Wang, Q. Ran, J. Ma, S. Yu, and L. Tan, "QRCI: A new quantum representation model of color digital images," vol. 438, p. 23775, 20 citations (INSPIRE 2023/12/24) 20 citations w/o self (INSPIRE 2023/12/24). [Online]. Available: https://www.sciencedirect.com/science/article/pii/S003040181930015X

[12] Y. Zhang, K. Lu, Y. Gao, and K. Xu, "A novel quantum representation for log-polar images," vol. 12, no. 9, pp. 3103–3126, 32 citations (INSPIRE 2023/12/24) 32 citations w/o self (INSPIRE 2023/12/24). [Online]. Available: http://link.springer.com/10.1007/s11128-013-0587-8

[13] F. Gray, "Pulse code communication," United States Patent 2632058, 1953.

[14] M. Möttönen, J. J. Vartiainen, V. Bergholm, and M. M. Salomaa, "Quantum circuits for general multiqubit gates," *Physical Review Letters*, vol. 93, no. 13, p. 130502, 2004.

[15] R. Potempa, O. Nwobodo, K. Wereszczynski, and K. Cyran, "General quantum image representation model and framework," 07 2024.

[16] W. Zhou and A. C. Bovik, "Mean squared error: Love it or leave it? a new look at signal fidelity measures," *IEEE Signal Processing Magazine*, vol. 26, no. 1, pp. 98–117, 2009.

[17] Q. contributors, "Qiskit: An open-source framework for quantum computing," https://qiskit.org, 2023.